

## On Interpolation in SPH

R. Vignjevic, T. De Vuyst, M. Gourma<sup>1</sup>

**Abstract:** The work presented provides an overview of different types of kernel interpolation used in the SPH method: conventional SPH, normalised SPH (NSPH), corrected kernel SPH (CSPH) and normalised corrected kernel SPH (NCSPH). These four methods are considered in a fully mesh-free form (using no background mesh). To illustrate the effect of using different interpolation methods two problems were simulated: a 1D symmetric elastic impact problem, and a shock-tube. An overview of the simulation results for the two problems is given. Shortcomings for the interpolation schemes tested were identified and discussed. It is concluded that NCSPH provides the best results. To establish whether the better results obtained with the NCSPH method are sufficient, or further improvements are needed, it will be necessary to conduct tests in two and three dimensions.

### 1 Introduction

The smoothed particle hydrodynamics method (SPH) is widely used in astrophysics and in gas dynamics simulations: Lucy(1977), Gingold and Monaghan(1977), Benz(1992), Monaghan(1982) and others. In the 1990's the method was extended to problems of solid mechanics including impacts: Libersky and Petschek(1993); Benz(1995); Johnson, Stryck, Beissel(1996); Swegle, Hicks and Attaway1994; Randles and Libersky(1996) and others. There are two significant reasons for increased interest in the SPH method. The first reason is the method's flexibility due to its Lagrangian and meshless nature, the second reason is that it works reasonably well when applied to problems in an unbounded domain. In a bounded domain, the SPH method still shows poor accuracy near boundaries. The issue of treatment of boundary conditions (e.g. free boundaries or interface tracking) in the SPH method is still in the domain of research [10], especially for NSPH and CSPH, both in hydrodynamic and material strength problems.

Recently, to remedy some of the problems, a series of studies developed by [Liu,Jun, Zhang(1995); Liu, Yun, Adee, Belytschko(1995); Liu, Chen(1995); Liu, Jun(1993)] introduced a polynomial correction function to the standard kernel function. This approach, called the 'Reproducing Kernel Particle Method' (RKPM) by the authors, seems to be able to handle material boundaries without losing consistency, and improving the accuracy of the solution.

In parallel to this a different type of correction was proposed by Johnson and Beissel(1996) and Randles and Libersky(1996). They suggest a normalization of the kernel sum in order to ensure that the derivative of a linear function is calculated exactly.

### 2 Basic Concepts and Equations

#### 2.1 Conventional SPH

The SPH method is based on the convolution principle or interpolant integral. Thus, any exact physical field (scalar, vector or tensor)  $\psi(x,t)$  depending on position vector  $x$  and on time  $t$  can be estimated by its smoothed value  $\langle \psi(x,t) \rangle$  given by

$$\langle \psi(x) \rangle = \int_{D_h W} \psi(s) \cdot W(x-s, h) \cdot ds \quad (1)$$

Where  $W(x-s, h) = W(z, h)$  is the kernel distribution,  $D_h W$  is the support of the kernel and  $h$  is a geometric parameter that defines size of the support also called the smoothing length.

$$\begin{aligned} D_h W &= \{z/z \in \mathfrak{R}^N, W(z, h) \in \mathfrak{R}^*\} \\ &= \{z/z \in \mathfrak{R}^N, z \in [-C \cdot h, +C \cdot h]\} \end{aligned} \quad (2)$$

Where  $C$  is a constant, the second equality is only valid for symmetric kernels. The kernel  $W(z, h)$  should possess the following properties:

<sup>1</sup> Cranfield University, Cranfield  
Bedford, UK

$$\int_{D_h W} W(x-s, h).ds = 1 \tag{3}$$

$$W(z, h) \xrightarrow{h \rightarrow 0} \delta_z \tag{4}$$

Where  $\delta_z$  is a Dirac function.

In numerical applications the integral in equation (1) is approximated by a pointwise integration:

$$\langle \psi(x_i) \rangle \approx \sum_{j \in N_i} \psi(x_j) \cdot W(x_i - x_j, h) \cdot \frac{m_j}{\rho(x_j)} \tag{5}$$

Where  $m_j$  is the mass associated with particle  $j$  and  $N_i$  is the set of particles interacting with the  $i$  particle, thus

$$N_i = \{j \in N / -C.h \leq x_i - x_j \leq C.h\} \tag{6}$$

The spatial derivative of  $\psi$  can be calculated using:

$$\langle \nabla \psi(x_i) \rangle \approx \sum_{j \in N_i} \psi(x_j) \cdot \nabla W(x_i - x_j, h) \cdot \frac{m_j}{\rho(x_j)} \tag{7}$$

Conventional SPH approximations, equations (5 and 7) as well as their variations [Libersky, Petch, et al.(1993); Benz(1995)], are inconsistent and unstable. As a consequence the accuracy of the approximations deteriorates near the boundaries (due to incomplete support) and with irregular particle distributions.

### 2.2 Normalized SPH

In order to correct for this problem the normalized SPH (NSPH) interpolation was introduced by Johnson and Biessel(1996), Randles and Libersky(1996) and Chen(1999) and consists of correcting the interpolation to compensate for irregular particle distributions and incomplete supports.

The condition that

$$\int_{D_h W \cap D} W(x-s, h).ds = 1 \tag{8}$$

is not satisfied if  $D_h W \not\subset D$ . In order to correct for this a correction factor  $C_0$  is introduced in the the normalisation condition so that:

$$C_0 \int_{D_h W \cap D} W(x-s, h).ds = 1 \tag{9}$$

Where  $C_0(x, h)$  is constant function with respect to  $s$  and determined by the normalisation condition, Using this approach the smoothed fields are given by

$$\langle \psi(x) \rangle \approx \frac{\int_{D_h W \cap D} \psi(s) \cdot W_{sph}(s-x, h).ds}{\int_{D_h W \cap D} W_{sph}(s-x, h).ds} \tag{10}$$

To approximate the gradients one can start from a semi-local Taylor series expansion  $\psi(s)$  about  $x$ :

$$\psi(s) \approx \psi(x) + (s-x) \cdot \langle \nabla_x \psi(x) \rangle + \frac{(s-x)^2}{2} \cdot \langle \nabla_x^2 \psi(x) \rangle + \dots \tag{11}$$

Multiplying the above equation by  $\nabla_s W_{sph}(s-x)$  and integrating over  $D_h W$  while ignoring second and higher order terms one gets:

$$\langle \nabla_x \psi(x) \rangle \approx \frac{\int_{D_h W} (\psi(s) - \psi(x)) \cdot \nabla_s W_{sph}(s-x, h).ds}{\int_{D_h W} (s-x) \cdot \nabla_s W_{sph}(s-x, h).ds} \tag{12}$$

The discrete forms of (10) and (12) are,

$$\langle \psi(x_i) \rangle \approx \frac{\sum_{j \in N_i} \psi(x_j) \cdot W_{sph}(x_j - x_i, h) \cdot \frac{m_j}{\rho_j}}{\sum_{j \in N_i} W_{sph}(x_j - x_i, h) \cdot \frac{m_j}{\rho_j}} \tag{13}$$

$$\langle \nabla_x \psi(x_i) \rangle \approx \frac{\sum_{j \in N_i} (\psi(x_j) - \psi(x_i)) \cdot \nabla_{x_j} W_{sph}(x_j - x_i, h) \cdot \frac{m_j}{\rho_j}}{\sum_{j \in N_i} (x_j - x_i) \cdot \nabla_{x_j} W_{sph}(x_j - x_i, h) \cdot \frac{m_j}{\rho_j}} \tag{14}$$

Two more remarks can be made regarding normalised SPH. The first one concerning the consistency of the approximation of the gradient. Due to the fact that higher order derivatives are neglected to obtain Eq. 12, this equation cannot be integrated to get  $\psi(x)$ .

The second problem is that even the integral forms of the normalised SPH equations (10)(12), unlike conventional SPH, does not satisfy the Gauss theorem.

### 2.3 Corrected SPH

The second type of correction was proposed by [Liu,Jun, Zhang(1995); Liu, Yun, Adee, Belytschko(1995); Liu, Chen(1995); Liu, Jun(1993)], and takes the following form as a correction to the interpolation kernel itself:

$$W_{\text{CSPH}}(x, x-s, h) = \left\{ \sum_{k=0}^M C_k(x, h) \cdot \left( \frac{x-s}{h} \right)^k \right\} \cdot W \left( \frac{|x-s|}{h} \right) \quad (15)$$

Where  $M$  is the order of the correction function and  $C_k(x, h)$  are coefficients that depend on the order  $M$ . These coefficients can be determined explicitly by imposing the condition that  $W_{\text{CSPH}}$  exactly interpolates polynomials of order up to  $M$ , i.e.

$$\int_{D_h W_{\text{CSPH}}} s^k W_{\text{CSPH}}(x, x-s, h) ds = x^k \text{ for } k = 0, 1, 2, \dots, M \quad (16)$$

Where  $D_h W_{\text{CSPH}}$  is the support of the CSPH kernel. In the results presented, a kernel correction of order  $M=1$  was used, hence:

$$W_{\text{cspH}}(x, s-x, h) = [C_1(x, h) + C_2(x, h) \cdot \left( \frac{s-x}{h} \right)] \cdot W_{\text{sph}}(s-x, h) \quad (17)$$

One can see that generally  $W_{\text{CSPH}}(x, x-s, h) \neq W_{\text{CSPH}}(s, s-x, h)$ , i.e. the kernel function is no longer symmetric.

Using the above a field can be approximated by:

$$\langle \psi(x_i) \rangle \approx \sum_{j \in Di} \psi(x_j) \cdot [C_1(x_i, h) + C_2(x_i, h) \cdot \left( \frac{x_j - x_i}{h} \right)] \cdot W_{\text{sph}} \cdot \frac{m_j}{\rho_j} \quad (18)$$

and consequently the gradient is approximated by

$$\langle \nabla_x \psi(x_i) \rangle \approx \sum_{j \in Di} \psi(x_j) \cdot [(C_1(x_i, h) + C_2(x_i, h) \cdot \left( \frac{x_j - x_i}{h} \right)) \cdot \nabla_x W_{\text{sph}} + \frac{C_2(x_i, h)}{h} \cdot W_{\text{sph}}] \cdot \frac{m_j}{\rho_j} \quad (19)$$

With the objective to preserve the Lagrangian and mesh-free nature of the method, a background mesh combined with Gauss quadrature, as proposed by Liu, was not used. Instead, a simple point-wise integration was used.

### 2.4 Normalized Corrected Kernel SPH

Finally, a combination of normalization and kernel correction was considered. The idea behind this is that the kernel correction restores consistency, while the normalization enhances accuracy of the integration process. The kernel function can then be written as:

$$W_{\text{ncsph}}(x, s-x, h) = [\hat{C}_1(x, h) + \hat{C}_2(x, h) \cdot \left( \frac{s-x}{h} \right)] \cdot \frac{W_{\text{sph}}(s-x, h)}{\int_{DW} W_{\text{sph}}(s-x, h) \cdot ds} \quad (20)$$

Where  $\hat{C}_1(x, h)$  and  $\hat{C}_2(x, h)$  are calculated by using a normalized kernel interpolation. A similar interpolation was proposed by Bonet and Kulasegaram (1998).

## 3 Velocity Smoothing

The velocity smoothing consists of applying a kernel interpolation to the velocity field. This process reduces or eliminates material inter-penetration and the fact that particles of the same material in a one-dimensional case can overtake each other. This type of procedure was published, in slight variations, by Libersky, Randles, Carney and Dickinson(1997); Guenther, Hicks, Swegle(1994 and Balsara(1995) as a potential cure for tensile instability. The formulation proposed by Randles, Libersky(1996) is as follows:

$$\tilde{v}_i = v_i + \alpha_{cs} \left[ \frac{\sum_{j \neq i}^{\text{nbr}} \frac{m_j}{\rho_j} v_j W_{ij}}{\sum_{j \neq i}^{\text{nbr}} \frac{m_j}{\rho_j} W_{ij}} - v_i \right] \quad (21)$$

Where  $\alpha_{cs}$  is the conservative smoothing coefficient and has a value between 0 and 1. The smoothing function for these tests is a variation of the above formula with  $\alpha_{cs} = 1$ , and including the  $i$ th particle in the kernel sum:

$$\tilde{v}_i = \frac{\sum_{j(\text{incl}i)}^{\text{nbr}} \frac{m_j}{\rho_j} v_j W_{ij}}{\sum_{j(\text{incl}i)}^{\text{nbr}} \frac{m_j}{\rho_j} W_{ij}} \quad (22)$$

One can see that this corresponds to a normalized SPH interpolation of a function. A second type of veloc-

ity smoothing that was considered is a Corrected Kernel SPH interpolation:

$$\tilde{v}_i = \sum_j^{\text{nbr}} \frac{m_j}{\rho_j} v_j \left( C_1 + C_2 \frac{x_j - x_i}{h} \right) W_{ij} \quad (23)$$

The use of velocity smoothing is an alternative to the use of artificial viscosity. An assessment of the performance of these two methods is given by Guenther, Hicks, Swegle(1994).

#### 4 Conservation Equations

As pointed out in [Gingold, Monaghan(1977); Benz(1992)] there are several formulations of the equations of motion in the SPH method. This is in part due to the fact that the kernels used are symmetric. This allows, without great difficulty, handling of conservation of momentum and energy. In the CSPH approach, due to the fact that the kernel is no longer symmetric, the possibilities of deriving an CSPH version of the equations of motion are restricted. In general let  $\psi(x_i, t)$  be any physical quantity carried by particle  $i$ ,  $\rho(s, t)$  and  $S(\sigma)$  be the density and a source term describing the state of the environment of that particle, its time derivative can then be expressed by:

$$\frac{d\psi(x_i, t)}{dt} = - \left\langle \frac{\vec{\nabla}_s S(\sigma)}{\rho(s, t)} \right\rangle_{s=x_i(t)} \quad (24)$$

In the case of the conservation equations:

$$\psi = \begin{pmatrix} 1 \\ \vec{v} \\ e \end{pmatrix} \text{ and } S(\sigma) = \begin{pmatrix} 0 \\ \sigma \\ \sigma : \vec{v} \end{pmatrix} \quad (25)$$

in this expression  $\vec{v}, e$  and  $\sigma$  represent material velocity, internal energy and the stress tensor. The system above is closed by an appropriate constitutive relation and compatibility equations. For conventional SPH the conservation equations are:

$$\frac{d\rho_i}{dt} = -\rho_i \sum_j \frac{m_j}{\rho_j} (v_j - v_i) \frac{\partial W_{ij}}{\partial x} \quad (26)$$

$$\frac{dv_i^\alpha}{dt} = \sum_j m_j \left( \frac{\sigma_j^{\alpha\beta} - q_j}{\rho_j^2} + \frac{\sigma_i^{\alpha\beta} - q_i}{\rho_i^2} \right) \frac{\partial W_{ij}}{\partial x^\beta} \quad (27)$$

$$\frac{dE_i}{dt} = \frac{\sigma_i^{\alpha\beta}}{\rho_i^2} \sum_j m_j (v_j^\alpha - v_i^\alpha) \frac{\partial W_{ij}}{\partial x^\beta} \quad (28)$$

Where  $q_i$  defines the artificial viscosity generated by the particle  $i$  and is given by.

$$q_i = \alpha \cdot \rho_i \cdot h \cdot C s_{ii} \cdot |Tr(\sigma_i)| + \beta \cdot \rho_i \cdot (h_i \cdot Tr(\sigma_i))^2 \begin{cases} 0 & \text{if } Tr(\sigma_i) < 0 \\ 0 & \text{if } Tr(\sigma_i) \geq 0 \end{cases}$$

and  $Tr(\sigma_i) = \sum_\alpha^{N \text{ dim}} \sigma_i^{\alpha\alpha}$ , where  $N \text{ dim}$  is the space dimension.

For the normalized SPH (NSPH) and corrected kernel SPH (CSPH) and normalized corrected kernel SPH (NCSPH) a different form of the momentum equation was used:

$$\frac{dv_i^\alpha}{dt} = -\frac{1}{\rho_i} \sum_{j \in N_i} m_j \left( \frac{\sigma_j^{\alpha\beta} - q_j - \sigma_i^{\alpha\beta} + q_i}{\rho_j} \right) \frac{\partial W_{\text{CSPH}}}{\partial x}(x_i - x_j, h) \quad (29)$$

This provides greater stability, this was also observed by Randles, Libersky(1996) and Balsara(1995). The reason for the improved stability is that if there is zero stress and a density discontinuity, equation (27) produces an acceleration, while equation (29) does not. It is important to note that throughout this paper only nodal integration has been used, in order to preserve the meshless character of the method.

#### 5 Test Results

To get an initial idea of the influence of these different methods on the interpolation a simple reconstruction of a function and its derivative was performed. The function to be reconstructed is a simple sine function, its derivative a cosine function.

From Figure 1 it can be seen that for a regular particle distribution the sine wave is reasonably approximated by

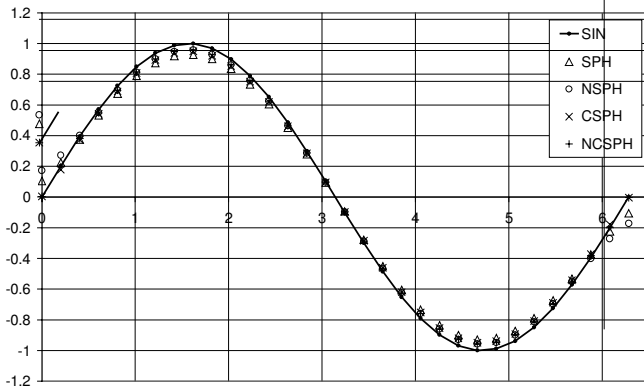


Fig. 1

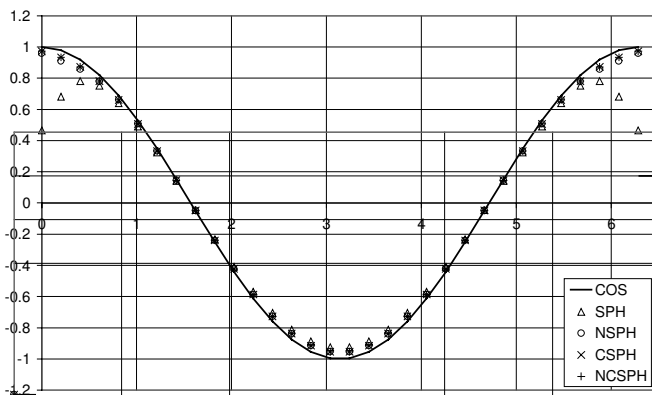


Fig. 2

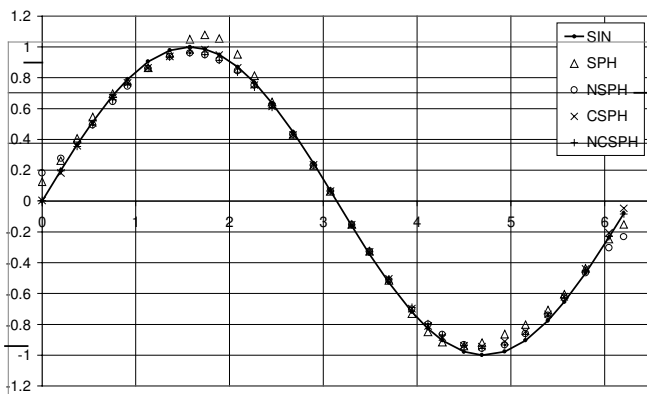


Fig. 3

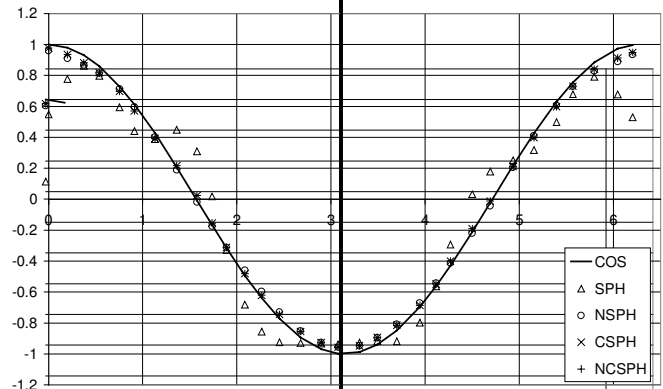


Fig. 4

all four methods, the CSPH and NCSPH methods also shows good results at the boundaries, conventional SPH and NSPH show a clear deficiency at the boundaries. Looking at the estimate of the derivative (Fig. 2) identical conclusions can be drawn, except that NSPH now has similar accuracy compared to CSPH and NCSPH.

The effect of irregular particle distributions (Fig. 3 and 4) the superiority of normalized and corrected kernel interpolations over the conventional SPH approach is clear. The conventional SPH results have clearly deteriorated. The results of NSPH, CSPH and NCSPH are hardly affected by the irregular distribution of particles. This confirms the fact that, as intended, NSPH compensates for the irregular particle distribution. Eventhough the rationale behind CSPH is a restoration of consistency it leads to a similar improvement as NSPH. These effects are even more noticeable when looking at the results of the approximation of the derivative of the sine function. The SPH results show virtually no resemblance to a cosine function.

Due to the nature of the problems to be analysed, ie. dynamics and wave propagation, a second function that was selected to be reconstructed is a step-function, and its derivative a Dirac function. The results for a regular particle distribution are displayed in Figures 5 and 6. Again one can observe the fact that NSPH, CSPH and NCSPH give better results at the boundaries. In the case of an irregular particle distribution (Fig. 7 and 8) it can be seen that the results for conventional SPH deteriorate, while the two other methods hardly are affected.

Finally, in the next four figures, the results of the reconstruction of a step function are presented using the parti-

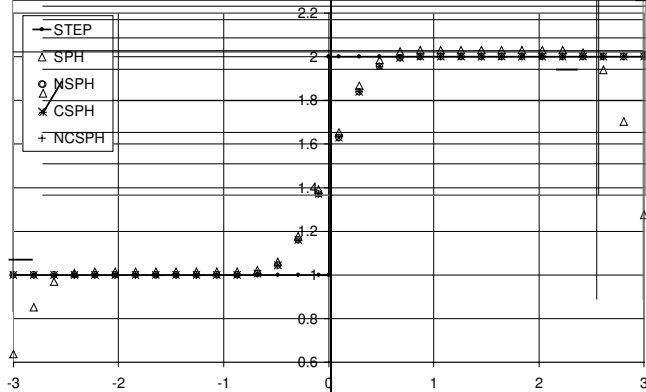


Fig. 5

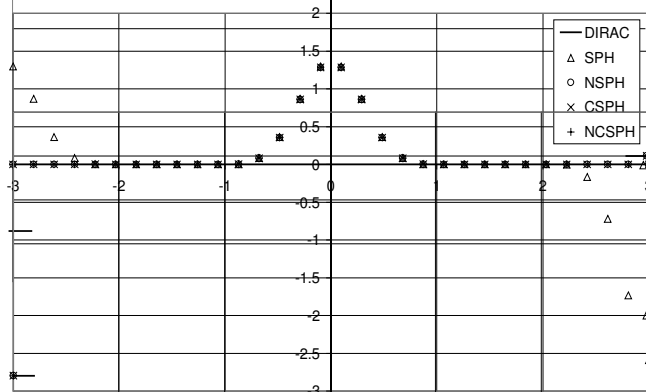


Fig. 6

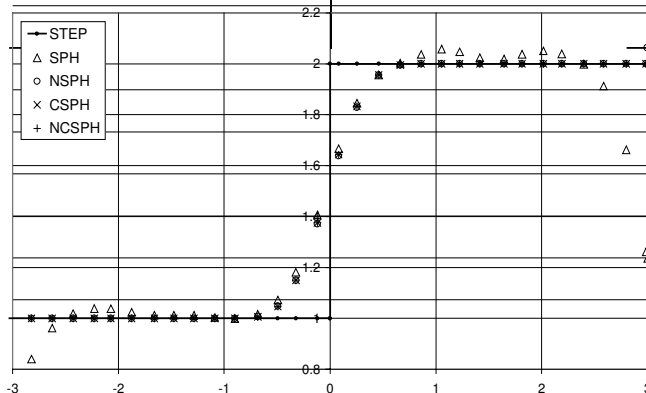


Fig. 7

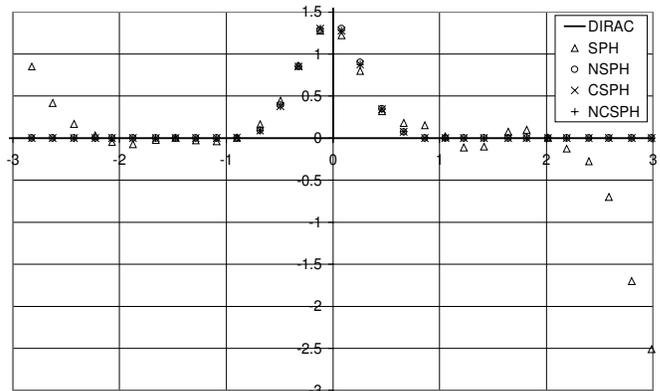


Fig. 8

cle distribution used to simulate the shocktube problem. The results of the shocktube problem will be discussed in a later paragraph. The main difference here is that to left of the origin the particle spacing is eight times denser than to the right. Consequently the volume of the particles also differs by a factor of eight. Conclusions drawn for the equal volume particle distribution case (Figures 5 to 8) also apply to non-equal volume case (Figures 9 to 10). The same calculation was also performed after a few timesteps, when the particles are no longer uniformly positioned, again the results are significantly worse for conventional SPH (Fig. 11-12).

To assess and compare the influence of the different interpolation methods on the discretisation of conservation methods two tests were conducted. For this study we have restricted ourselves to one dimensional problems.

The first problem that was selected to study the different interpolation methods is a 1D symmetric elastic impact of two bars. The initial problem configuration is summarized in the Table 1 below.

Table 1

Parameter	Value
Number of Particles	4000
Number of Materials	2
Particle Spacing $\Delta$	0.05 cm
Smoothing Length $h$	0.05 cm
Young's Modulus $E$	200Gpa
Poison's Ratio	0.3
Impact velocity	+/- 100 m/s

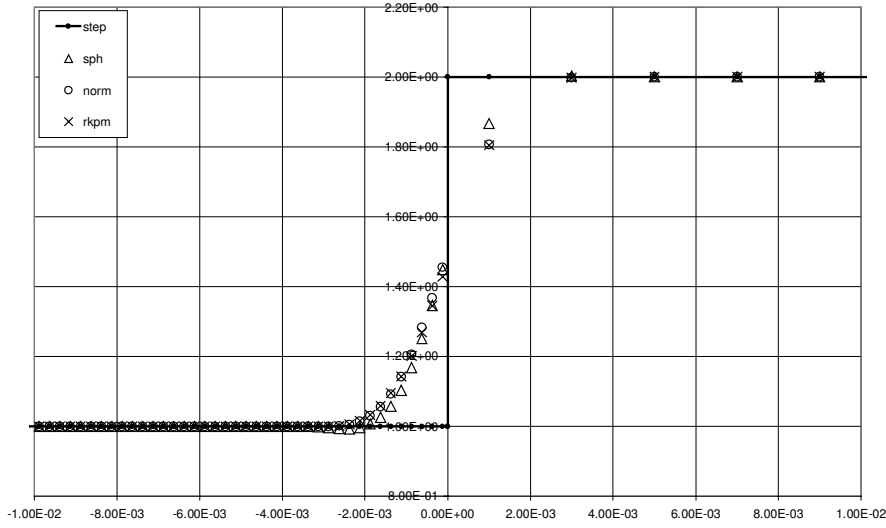


Fig. 9

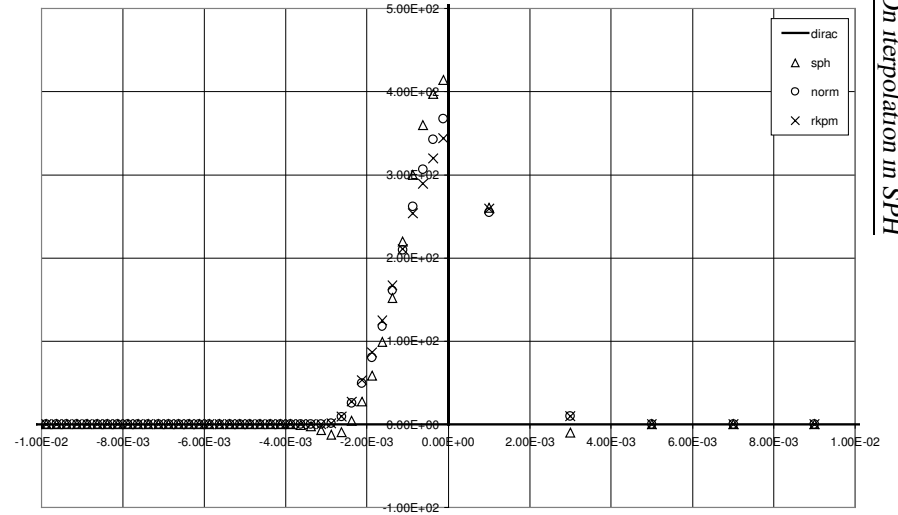


Fig. 10

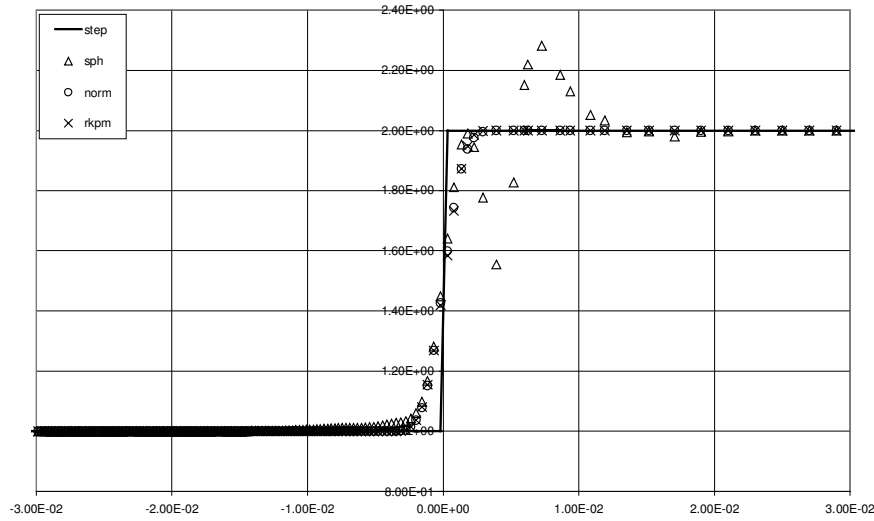


Fig. 11

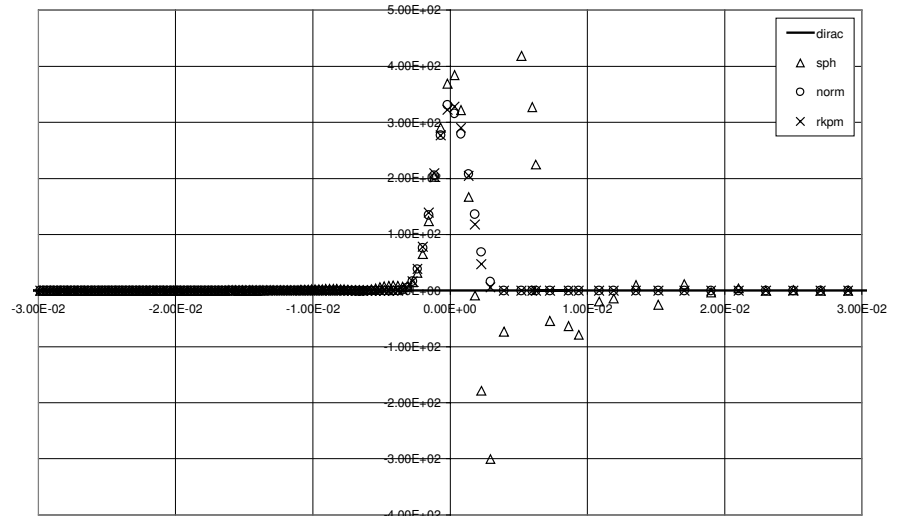
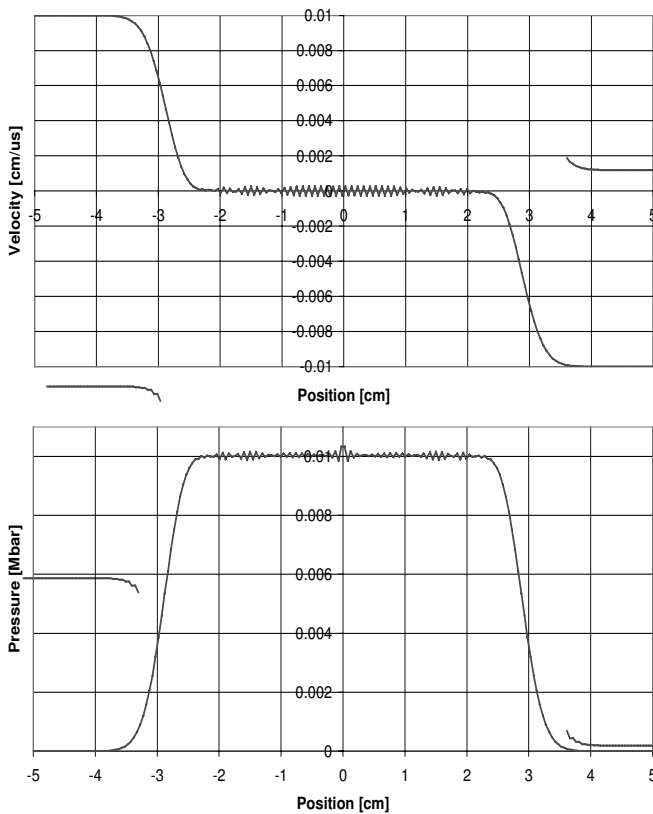


Fig. 12

Unless otherwise indicated the units used throughout this paper are: cm, g,  $\mu$ . The results are presented for a time  $10\mu$  after impact. Ideally the velocity behind the stress waves should be equal to zero, in the case of conventional SPH there is oscillation behind the stress- and velocity-wave which is a consequence of the numerical approach used. The oscillation is present in the region behind the stresswave as can be seen from Fig. 13. In the case of normalized SPH and corrected kernel SPH and normalized corrected kernel SPH one can see that there are no oscillations (Figures 14 to 16).



**Figure 13 :** Velocity and Pressure  $10\mu$  after Impact using Conventional SPH Interpolation

The second problem that was selected for this test is a shocktube problem. The shocktube problem is a widely used test case to validate numerical algorithms for the simulation of hydrodynamic problems [Sod(1978)]. The reason for its popularity is that the solution contains large density differences, and that several discontinuities, in the form of shockfronts, are present. For these reasons, and the inherent inability of SPH to deal with large density differences, the shocktube problem was selected as a

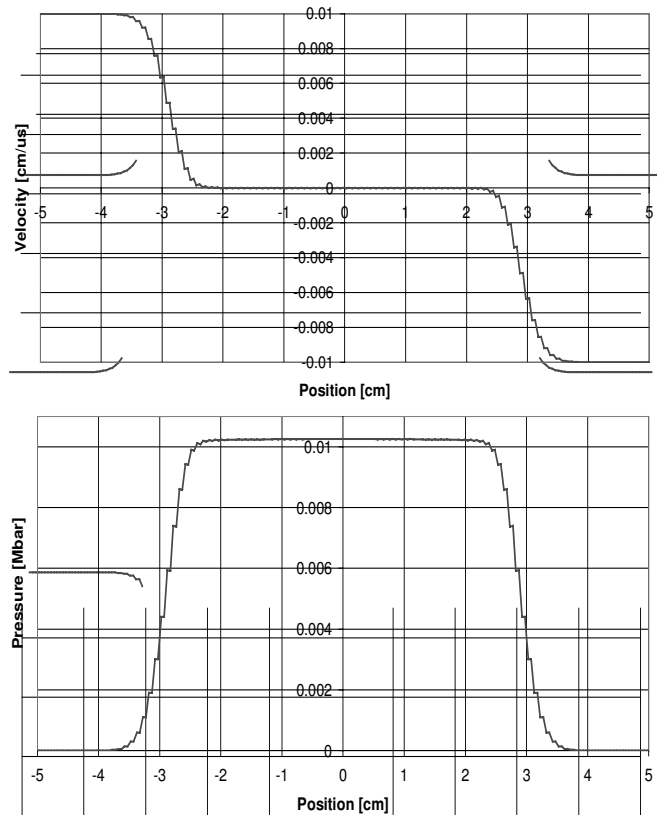


**Figure 14 :** Velocity and Pressure  $10\mu$  after Impact using normalized SPH Interpolation

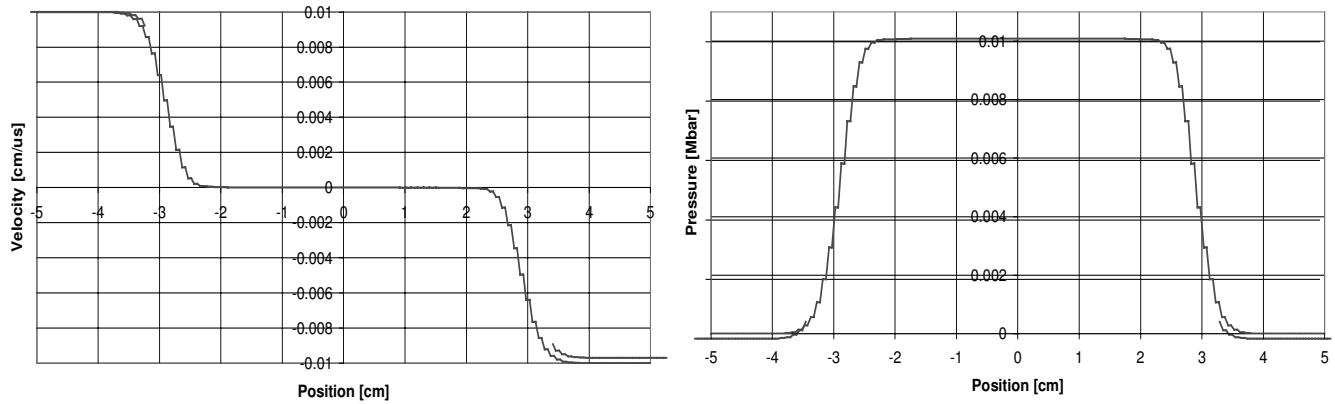


**Figure 15 :** Velocity and Pressure  $10\mu$  after Impact using Corrected Kernel SPH Interpolation

test case.

The basic setup of the shocktube problem are two tubes of gas. One of the gasses has a high density, pressure and internal energy, while the other has low density, pressure and internal energy. The initial velocities of the both gasses is zero.

In practice the gasses are separated by a diaphragm. After the diaphragm is removed the low density gas is compressed resulting in a shockwave propagating to the right, the high density gas expands to the right with an expansion wave travelling to the left (see Fig.17). The difficulty lies in accurately simulating the resulting compression and expansion waves, as well as obtaining accurate values for pressure, density, velocity and internal energy.

The problem that was used to test our SPH code has the characteristics summarized in Table 2:

**Table 2:** Initial Conditions of Shocktube Problem

Parameter	High Density Gas	Low Density Gas
Density $\rho$ [g/cm <sup>3</sup> ]	1.0	0.125
Pressure $p$ [mbar]	1.0	0.1
Velocity $v$ [km/s]	0.0	0.0

The material model used was an ideal gas with the equation of state given below:

$$p = \rho(\gamma - 1)e \tag{30}$$

In this case a value for  $\gamma$  1.4 was used for both gasses. The analytical solution was calculated using the method described in [Toro(1997)]. The results are shown for a time of  $0.25\mu$  after breaking the diaphragm (Fig. 17), and are summarized in Table 3. The different sections correspond to a change in value of one of the variables

- velocity, density or pressure - through the solution domain, from left to right. The values for section 2 are omitted as the variables are not constant in that section.

The particles were distributed over the domain such that the mass of each particle was the same. As a result of this the mesh density in the high density gas was higher (ie. particles are closer together) than the low density gas. This results 4000 particles in the high density part of the gas, 500 for the low density gas.

The solution obtained with a conventional SPH procedure compares very well with the analytical solution, but exhibits a significant amount of oscillation through the solution domain. Furthermore one can observe a spike in all three plots at the point of contact between the two gasses (Figures 18, 19 & 20). These oscillations are caused by the fact that the particles of the two gasses mix around the contact area, and the particles of the same gas change order.

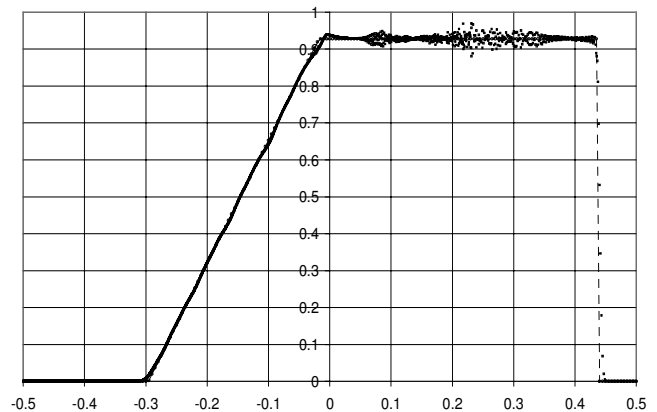


**Figure 18 :** Velocity Profile after  $0.25\mu$  using Conventional SPH

**Table 3 : Analytical Solution of Shocktube Problem**

Parameter	Section 1	Section 2	Section 3	Section 4	Section 5
Density $\rho$ [ $\text{g/cm}^3$ ]	1.0	Gradient	0.4263	0.2656	0.125
Pressure $p$ [mbar]	1.0	“	0.3031	0.3031	0.1
Velocity $v$ [km/s]	0.0	“	0.9275	0.9275	0.0

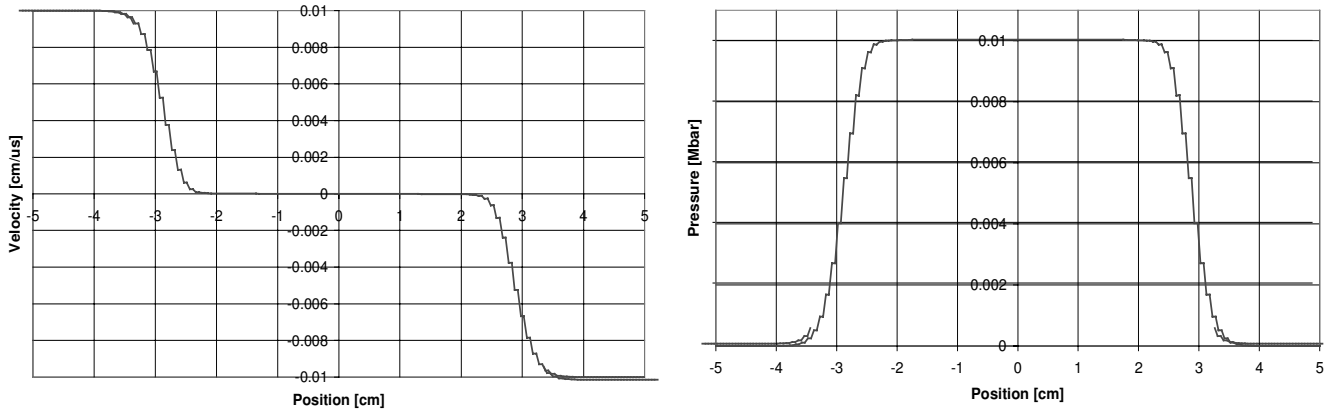


**Figure 16 : Velocity and Pressure  $10\mu$  after Impact using normalized Corrected Kernel SPH Interpolation**

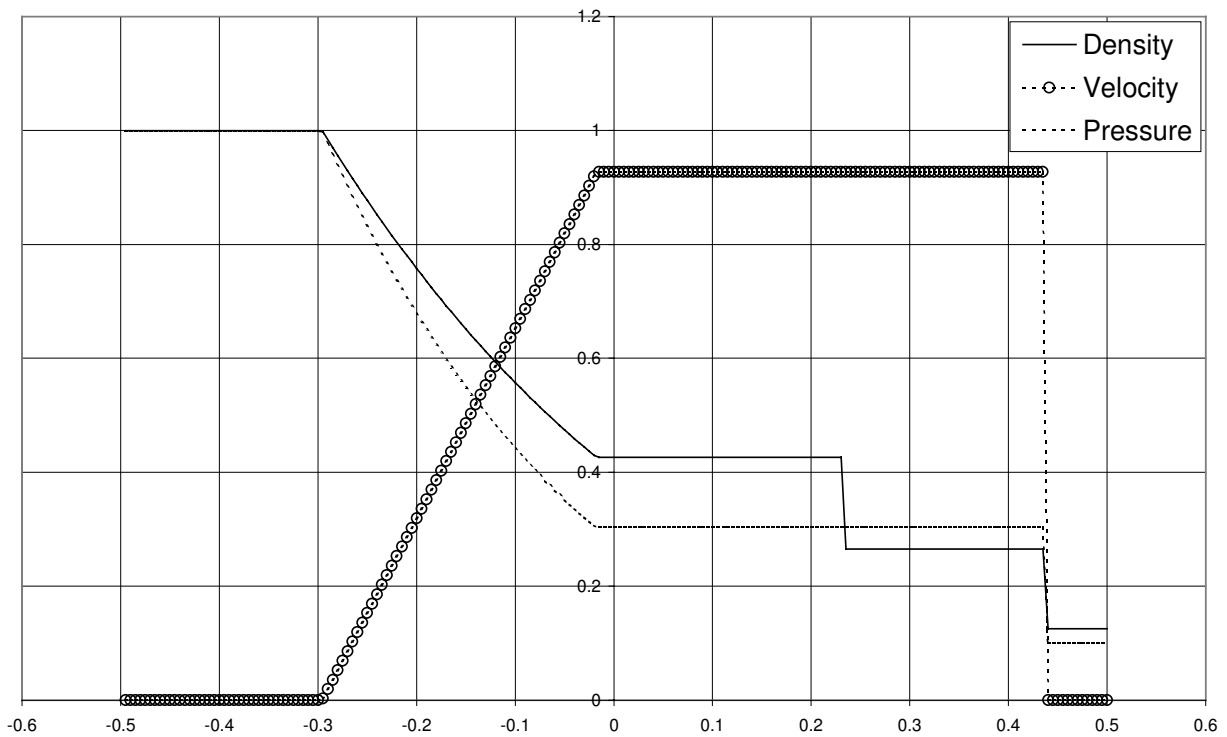


**Figure 17 : Analytical Solution of Shocktube Problem**

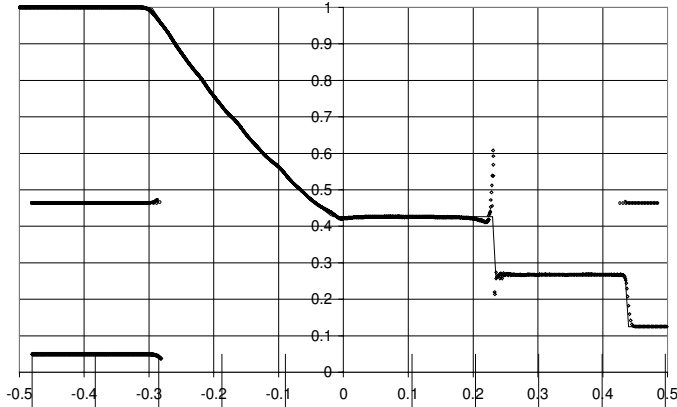


Figure 19 : Density Profile after  $0.25\mu$  using Conventional SPH

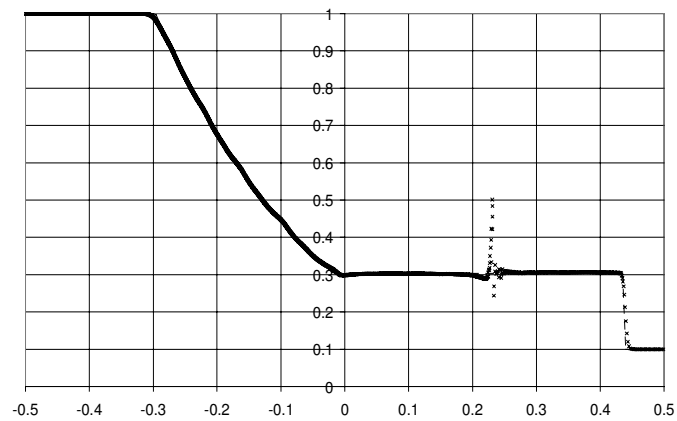


Figure 20 : Pressure Profile after  $0.25\mu$  using Conventional SPH

The normalized SPH test case crashes after about ten timesteps, this is due to the fact that particles of the expanding gas overtake each other and that a large gap forms between the two gasses after one timestep. Due to the latter effect a neighbour deficiency develops for the particles at the point of contact of the two gasses. This causes the normalization factor of Equation 13:

$$\sum_j^{\text{nbr}} \frac{m_j}{\rho_j} (x_j - x_i) \frac{dW_{ij}}{dx} \quad (31)$$

to become significant, and hence to result in a large correction to the calculation of gradients compared to conventional SPH. In this case this affects the calculation of the strain rate and accelerations.

Due to the time integration method used, the central difference scheme, the first variable to change after the problem initialisation stage is the acceleration.

If one compares the values that are calculated for the accelerations during this first timestep (Figure 21) one sees that for the high density gas the accelerations are very similar, but for the low density gas there is a significant increase in acceleration due to the normalized SPH interpolation. This is related to the fact that the kernel support contains less particles. A similar effect can be observed for Corrected Kernel SPH (CSPH) but these results will be discussed in a later paragraph.

The next steps in the solution process are updating velocities and positions. Due to the large difference in accelerations left and right of the contact point between the two gasses the low density particle will move a lot further than the high density particle. Hence the formation of a large gap between the two gasses. Furthermore one can see that the acceleration for the second low density particle is a lot lower than the first one. This results in those two particles being very close together after the first timestep. This means that there is a discrepancy between the volume occupied by the particles (for example the volume half-way to the next particle in 1D) and the values of  $V_j = m_j/\rho$  the nodal volumes or integration weights. To alleviate this problem velocity smoothing was applied at every timestep. Four combinations were initially considered: SPH, NSPH and CSPH and NCSPH with velocity smoothing using a normalized kernel interpolation (Eq. 7).

Applying the velocity smoothing (VS) to the conven-

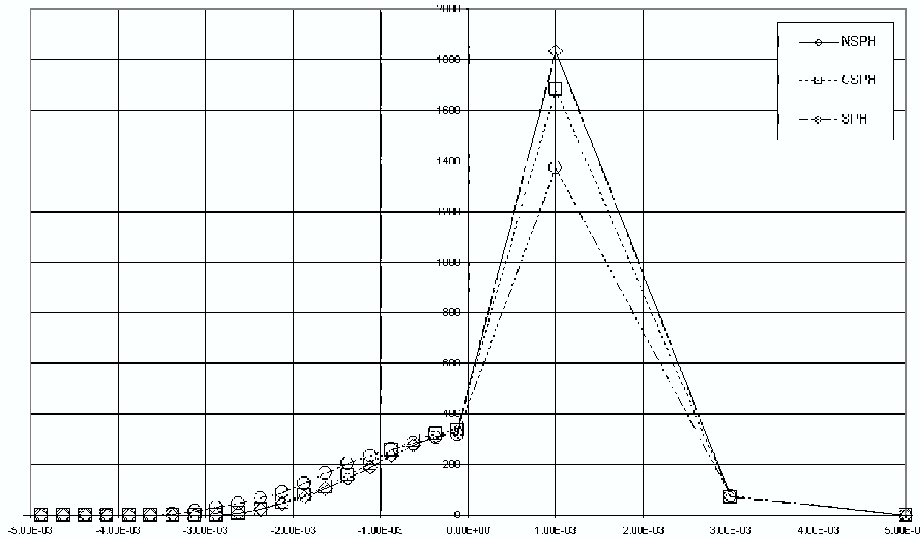


Figure 21 : Accelerations during the first timestep.

tional SPH solution results in a solution without significant oscillation, especially the oscillations in the velocity field are much improved (Figure 22), apart from the obvious effect of slightly higher dispersion. There is however still a spike at the contact between the two gasses in the density and pressure field (Figures 23 & 24). This is despite the fact that the velocity smoothing prevents particle interpenetration, and the particles remain more or less evenly distributed, even around the contact point. This is probably due to the fact that if one smooths the velocities then these values will no longer be consistent with, for example, the density, pressure or specific internal energy fields. More work is required to investigate possible solutions for this problem. Of course an explicit modelling of the contact between the gasses, such as in [Campbell, Vignjevic, Libersky(2000)], would solve interpenetration problems, but could in turn cause oscillations at the contact in the form of chatter between the contact nodes. Furthermore, contrary to what was hoped the gradients of the velocity, density and pressure fields are not zero between the expansion and compression waves.

In the case of NSPH with normalized velocity smoothing the main observation is that the problem runs in a stable way. This confirms the fact that NSPH is unable to cope with such high density and pressure discontinuities because of particle interpenetration. Unfortunately the results are significantly worse than the SPH ones as can be seen in Figures 25 to 27. The velocity between the expansion and compression waves is far from constant,

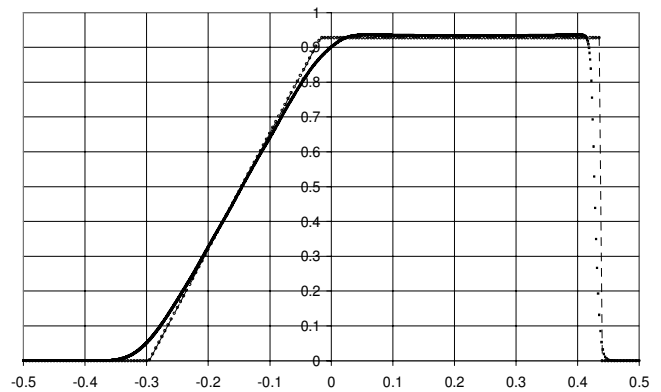


Figure 22 : Velocity Profile using Conventional SPH w. NVS

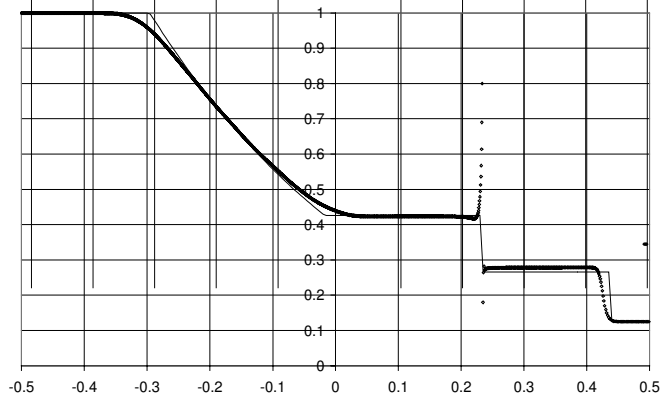
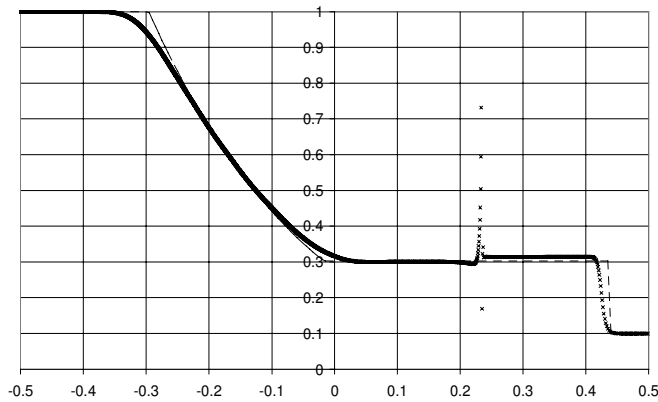
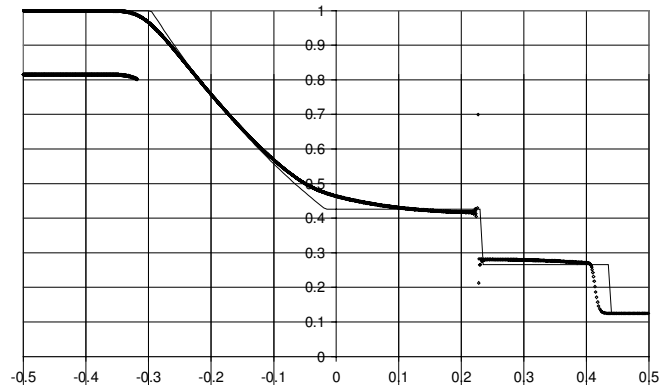


Figure 23 : Density Profile using Conventional SPH w. NVS



**Figure 24 :** Pressure Profile using Conventional SPH w. NVS



**Figure 26 :** Density Profile using NSPH w. NVS

almost like a parabolic curve. The density and pressure are slanted rather than horizontal. The reason for this behaviour is not immediately clear, but may be related to the fact that normalized SPH can only calculate linear gradients exactly. Furthermore one can notice that there is a significant lag of the shockfront.

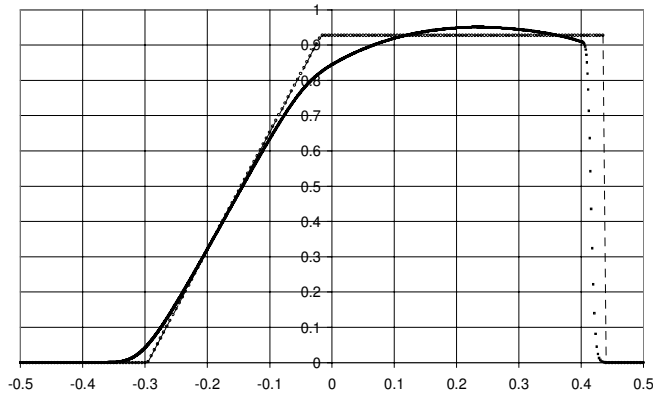


**Figure 25 :** Velocity Profile using NSPH w. NVS

The results of the NSPH analysis with velocity smoothing using a reproducing kernel interpolation (Eq. 8) show similar behaviour to the normalized velocity smoothing (Fig. 28 – 30). The velocity field between the shock-fronts appears to be in this case, piecewise linear, as opposed to the curved shape in the normalized velocity smoothing (NVS). Other than that, similar observations can be made: the density and pressure fields are slanted, and there is a lag in the compression wave front.

The simulation results of the CSPH analyses with velocity smoothing are shown in Figures 31 to 36. Again the

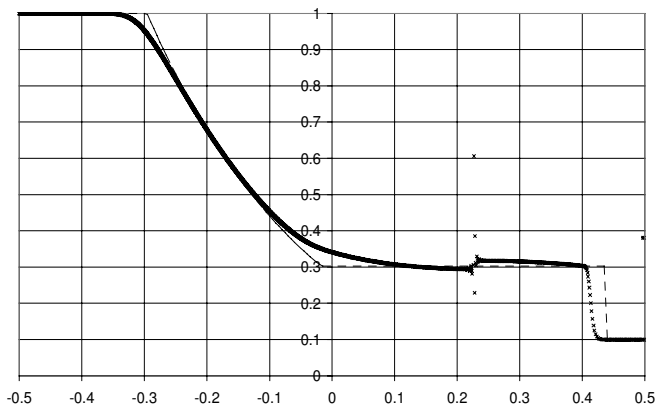


**Figure 27 :** Pressure Profile using NSPH w. NVS

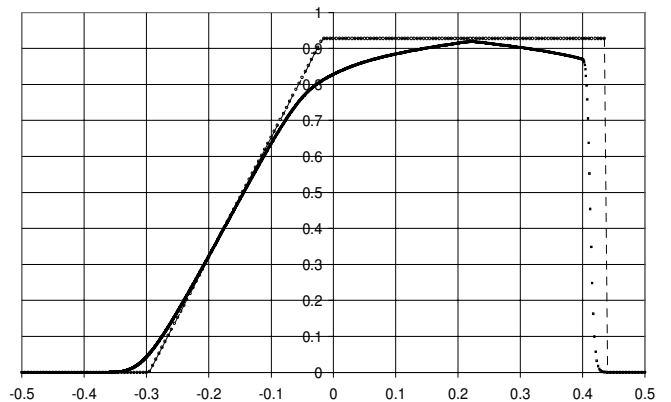


**Figure 28 :** Velocity Profile using NSPH w. CVS

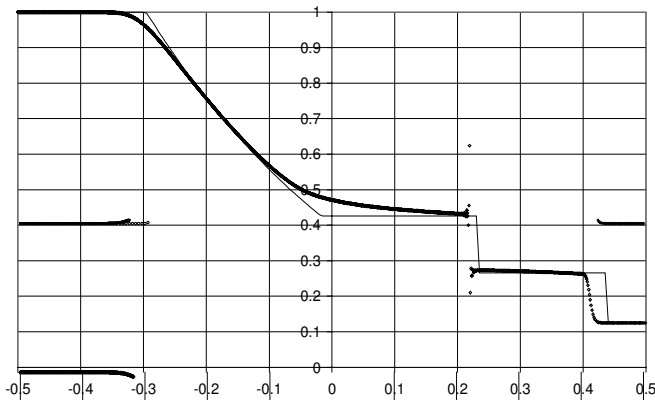


Figure 29 : Density Profile using NSPH w. CVS

first observation is that using the velocity smoothing the problems run without error termination because particle mixing is prevented. Similar to the NSPH results with velocity smoothing there is an error in the propagation speed of the compression wave. On top of that the values that are obtained for the velocity, density and pressure fields between the wave fronts show a noticeable error. The effect of the fields being slanted is far less exaggerated but still present. The combination of CSPH with CVS gives marginally superior results over CSPH with NVS. Again there is a spike at the contact between the two gasses in the density and pressure fields.

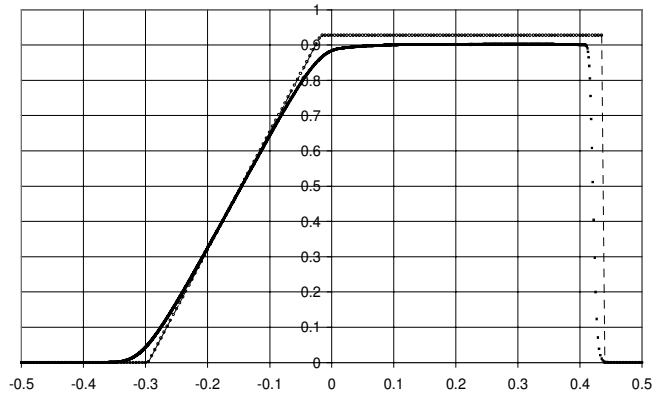


Figure 31 : Velocity Profile after  $0.25\mu$  using CSPH w. NVS

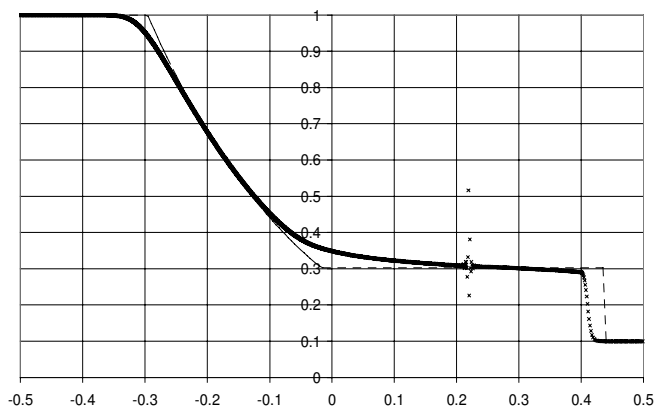


Figure 30 : Pressure Profile using NSPH w. CVS

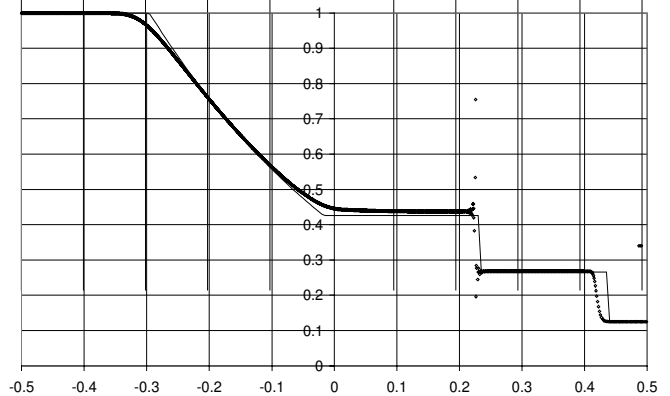
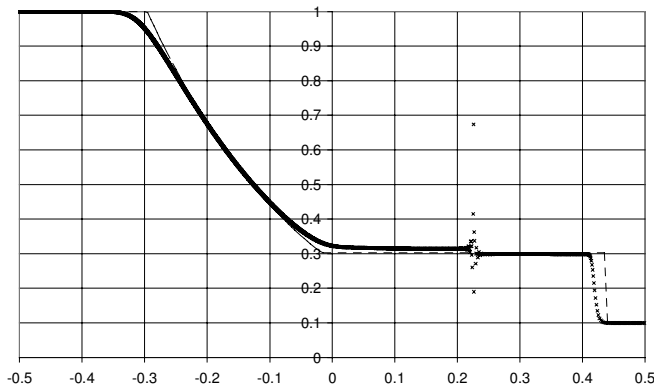


Figure 32 : Density Profile after  $0.25\mu$  using CSPH w. NVS

The velocity, density and pressure profiles obtained by NCSPH are shown in Figures 37 to 39 and are much better than the profiles calculated using the other methods. This, first of all, shows that the improved integration due



**Figure 33** : Pressure Profile after  $0.25\mu$  using CSPH w. NVS

to the normalization stops the simulation crashing. This indicates that it necessary for the correction constants to be evaluated very accurately and that a simple nodal integration is insufficient. The NCSPH results compare well with the analytical solution and those obtained by SPH method. But one can see that the oscillations behind the shock are not as pronounced as the conventional SPH results, compare Figures 18 and 37. The density and pressure graphs show good resolution of the shocks. The spike at the contact point between the two gasses present in all the other results is not as prominent in this case.

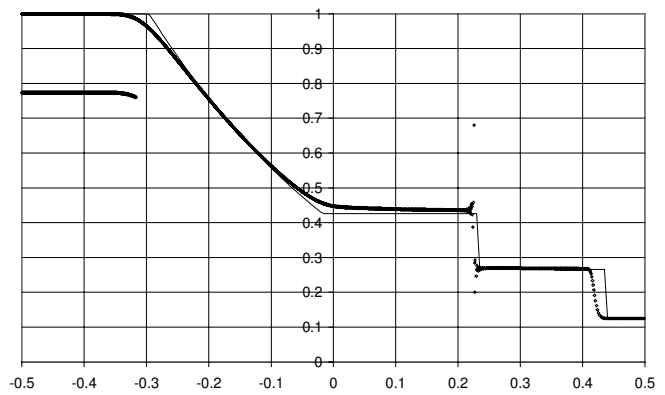


**Figure 35** : Density Profile after  $0.25\mu$  using CSPH w. CVS

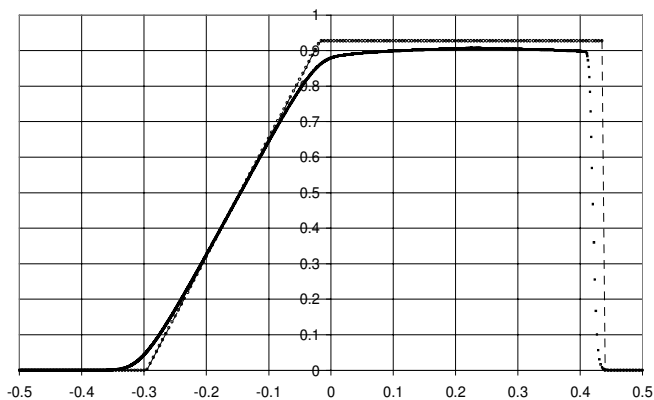


**Figure 34** : Velocity Profile after  $0.25\mu$  using CSPH w. CVS

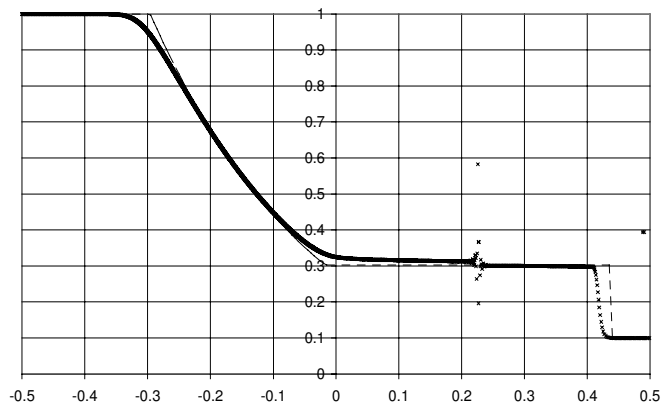


**Figure 36** : Pressure Profile after  $0.25\mu$  using CSPH w. CVS

Finally the combination of NCSPH with velocity smoothing was tested. The results are very good with very little oscillation, but the velocity smoothing introduces an error in wave propagation speed.

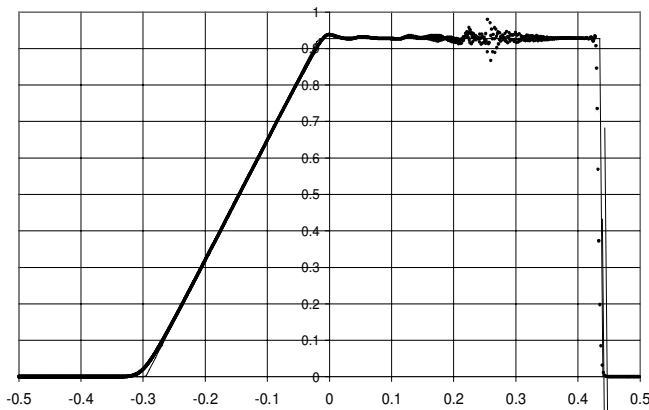


Figure 37 : Velocity Profile after  $0.25\mu$  using NCSPH

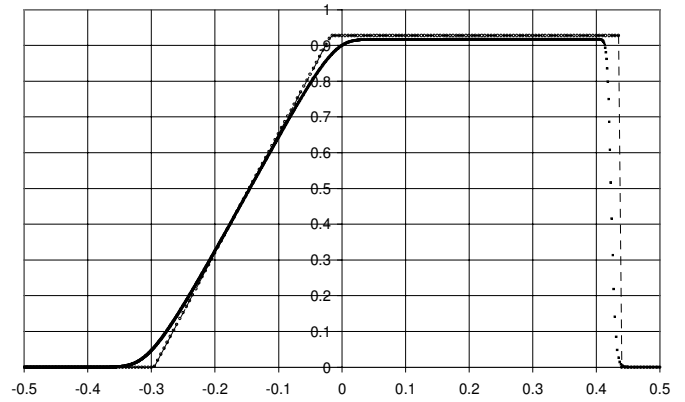


Figure 40 : Velocity Profile after  $0.25\mu$  using NCSPH with VS

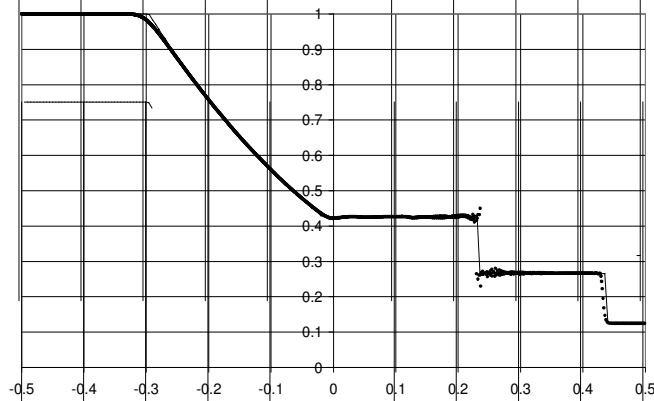


Figure 38 : Density Profile after  $0.25\mu$  using NCSPH

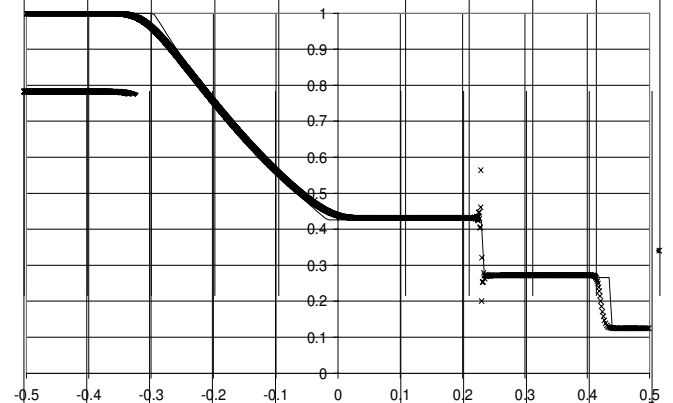


Figure 41 : Density Profile after  $0.25\mu$  using NCSPH with VS

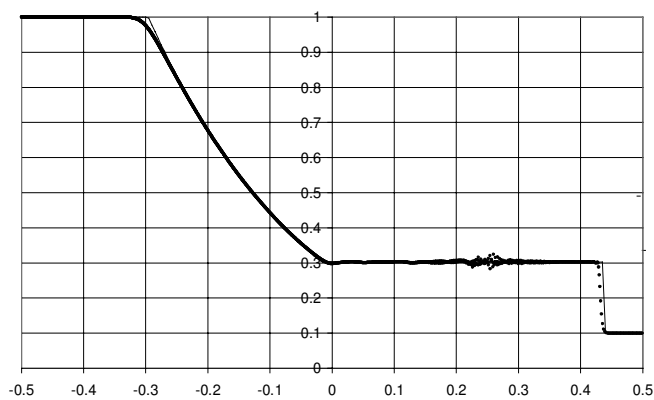


Figure 39 : Pressure Profile after  $0.25\mu$  using NCSPH

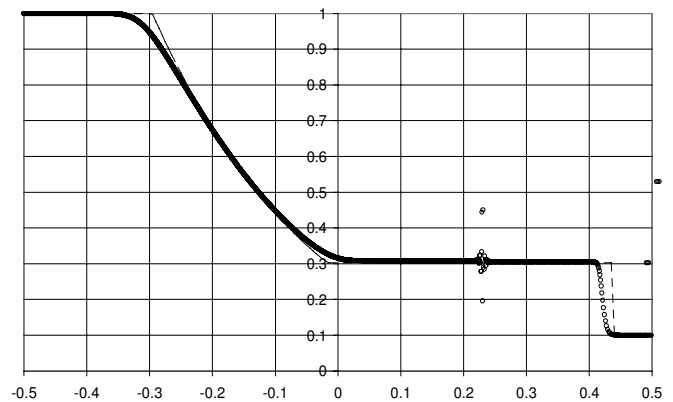


Figure 42 : Pressure Profile after  $0.25\mu$  using NCSPH with VS

## 6 Discussion

From the conducted tests it can be concluded that for the reconstruction of functions and their derivatives the normalized, corrected kernel and normalized corrected kernel SPH significantly improve the results compared to those obtained with conventional SPH.

From the results of the elastic impact problem one can conclude that again the results show an improvement in that the oscillations present in the SPH solution are eliminated.

For the more severe test of a shocktube simulation the balance is slightly shifted. The conventional SPH results are accurate, but show a large amount of oscillation. These oscillations can be filtered out by applying velocity smoothing at the cost of a slightly less accurate solution because of the dispersion it causes.

The NSPH and CSPH methods can not handle the large variations and discontinuities in the field variables. So, despite improving the quality of the interpolation they perform significantly worse than conventional SPH. The combination of kernel normalization, or corrected kernels, with nodal integration is unstable if large density differences are present and the grid becomes irregular. This has been reported in several other papers such as Voth, Christon(2001) and Christon, Voth(2000). It is interesting to note that SPH, despite the inaccuracy of the interpolation does not suffer from this. Using velocity smoothing solves this problem only to an extent as the solutions are stable but not very accurate. There is an error in wave propagation speed, and there are significant errors in the values obtained for the field variables between the shocks. The profiles exhibit slopes which are amplified as simulation proceeds, hence, the method is unstable. One probable reason is the lack of a direct relation between a field and its gradients, and that the equations 10 and 12 do not satisfy Gauss/Ostrogradsky theorem. Normalized and corrected kernel velocity smoothing give similar results, the latter performing slightly better.

The best results are obtained using by the NCSPH method, the oscillations present in the SPH solution are far less pronounced in this case. Also the magnitude of the spike at the contact point between the two gasses is reduced. Adding velocity smoothing to NCSPH completely eliminates oscillations in the velocity field, and reduces those in the density and pressure fields, at the cost of an error in wave propagation speed.

## 7 Conclusion

From the conducted tests one can conclude that NCSPH performs the best. There is less oscillation in the solution than conventional SPH, and it can handle the discontinuities of a shocktube problem. This last problem is where NSPH and CSPH fail, despite showing good results for elastic impact problems.

The use of velocity smoothing provides a stabilising factor and reduces oscillations. The disadvantage is the dispersion and error in wave propagation speed it causes.

To establish whether the improvement in results obtained using the NCSPH method is sufficient or further improvements are needed it will be necessary to conduct tests in two and three dimensions.

## References

- Balsara D. S. (1995): "Von Neumann stability analysis of Smooth Particle Hydrodynamics suggestions for optimal algorithms". *J. Comp. Phys*, 121, 357-372.
- Benz W. (1992): "Smooth Particle Hydrodynamics" *Ann. Rev. Astro. Astroph.*, 30, 543-74.
- Benz W. (1995): "Simulation of Brittle Solids using Smoothed Particle Hydrodynamics", *Comput. Phys. Comm.*, Vol. 87, 253-265.
- Bonet J., Kulasegaram S. (1998): "Correction and Stabilisation of Smoothed Particle Hydrodynamics with Applications in Metal Forming Simulations", CR/985/98, University of Wales, Swansea.
- Campbell J., Vignjevic R., Libersky J.L (2000): "A Contact algorithm for Smooth Particle Hydrodynamics", *Comput. Methods. Appl. Mech. Engrg.*, Vol. 184,67-85
- Chen J.K. (1999): "A Corrective Smoothed Particle Method for Boundary Value Problems in Heat Conduction", *Int. J. Num. Meth. Engrg.*, Vol. 46, 231-252.
- Christon M., Voth T. (2000): "Results of Von Neumann Analyses for Reproducing Kernel Semi-Discretisations", *Int. J. Num. Meth. Engrg.*, Vol. 47, 1285-1301.
- Gingold R.A., Monaghan J.J, (1977): *Mon. Not. R. Astr. Soc.*, 181, 375-389.
- Guenther C., Hicks D. L., and Swegle J. W. (1994): "Conservative Smoothing versus Artificial Viscosity", Technical Report SAND94-1853, Sandia National Laboratory.

- Johnson S., Stryck R., Beissel S. (1996): "SPH for High Velocity Impact Computations", *Comp. Meth. Appl. Mech. Engrg.*, Vol 139, 347-373.
- Johnson G., Beissel S. (1996): "Normalized Smoothing Functions for SPH impact Computations", *Int. J. for Num. Meth. in Engrg*, Vol. 39, 2725-2741.
- Libersky L., Petchek A. et al (1993): "High Strain Lagrangian Hydrodynamics", *J. Comput. Phys.*, 109, 67-75.
- Libersky L., Randles P., Carney T., Dickinson D. (1997): "Recent Improvements in SPH modelling of Hypervelocity Impact", *Int. J. Impact Engng*, 20, 525-532.
- Liu W., Chen Y. (1995): "Wavelet and Multiple Scale Reproducing Kernel Methods", *Int. J. of Num. Meth. in Fluids*, Vol. 21, 901-931.
- Liu W., Jun S. (1993): "Reproducing Kernel Particle Methods for Elastic and Plastic Problems", *Adv. Comp. Meth. for Material Modeling*, AMD-Vol 180, 175-189.
- Liu W., Jun S., Zhang Y. (1995): "Reproducing Kernel Particle Methods", *Int. J. of Num. Meth. in Fluids*, Vol. 20, 1081-1106.
- Liu W., Yun S., Li S., Adee J., Belytschko T. (1995): "Reproducing Kernel Particle Methods for Structural Dynamics", *Int. J. Num. Meth. Engrg.*, 38, 1655-1679.
- Lucy L. (1977): "A Numerical Approach to the Testing of the Fission Hypothesis", *The Astronomical J.*, 82, 1013-1024.
- Monaghan J.J. (1982): "On the Problem of Penetration in Particle Methods", *J. of Comp. Phys.*, 82, 1-15.
- Randles P., Libersky L. (1996): "Smoothed Particle Hydrodynamics: Some Recent Improvements and Applications", *Comp. Methods Appl. Mech. Engrg.*, Vol. 139, 375-408.
- Sod G. A. (1978): "A Survey of Several Finite Difference Methods for Systems of Nonlinear Hyperbolic Conservation Laws", *J. Comput. Phys*, 27, 1-31.
- Swegle J., Hicks D., Attaway S. (1994): "An Analysis of Smoothed Particle Hydrodynamics", *SAND93-2513*, Sandia National Laboratories, Albuquerque.
- Toro E. F.(1997): "Riemann Solvers and Numerical Methods for Fluid Dynamics", Springer, pp152-157.
- Voth T., Christon M. (2001): "Discretisation errors associated with reproducing kernel methods: one-dimensional domains", *Comp. Meth. Appl. Mech. Engrg*, Vol. 190, 2429-2446.